Journal of Materials Chemistry A

COMMUNICATION

View Article Online
View Journal | View Issue

Cite this: J. Mater. Chem. A, 2015, 3, 19674

Received 7th August 2015
Accepted 29th August 2015

DOI: 10.1039/c5ta06172e

www.rsc.org/MaterialsA

Hydrochloric acid accelerated formation of planar $CH_3NH_3PbI_3$ perovskite with high humidity tolerance†

Ge Li,‡ Taiyang Zhang‡ and Yixin Zhao*

We demonstrate high humidity tolerant one-step and sequential deposition methods to fabricate high quality planar $CH_3NH_3PbI_3$ perovskite films with the assistance of HCl. The addition of stoichiometric HCl into PbI_2 precursor solution from 33 wt% hydrochloric acid leads to the formation of a novel $HCl{\cdot}PbI_2$ precursor film, which can be easily thermally decomposed back into PbI_2. This novel intermediate planar $HCl{\cdot}PbI_2$ precursor film can be completely converted into a compact planar $MAPbI_3$ film within only 10 s at room temperature *via* sequential deposition. In another novel one step method the precursor solution of PbI_2 + MAI + HCl obtained by adding stoichiometric HCl into regular PbI_2 + MAI precursor solution was used to fabricate a very smooth planar $MAPbI_3$ film by just spin coating. Both the one step and sequential deposition methods can be used to fabricate high quality planar perovskite films in a hood under ambient conditions with up to 60% humidity level for high efficiency planar perovskite solar cells.

Introduction

Organometallic halide perovskite solar cells have become one of the most promising candidates for the realization of low-cost, high-efficiency solar cells. Within the past 3 years, the efficiency of solid state perovskite solar cells has increased to more than 20% from an initial value of ~10% and is still increasing.[1–7] Solution chemistry approaches are highly facile and effective for the deposition of high quality perovskite films.[8] Currently, there are two main popular solution chemistry synthesis routes for perovskite deposition. The first approach is a one-step solution process *via* direct spin coating of different kinds of perovskite precursor solutions with or without additives onto the substrate, followed by thermal annealing or solvent engineering to crystallize the perovskite film.[9–15] The second most popular and commonly used synthetic approach is a two-step sequential deposition,[4,16] in which a precursor film of PbI_2 is first deposited onto the substrate followed by the conversion of PbI_2 into $CH_3NH_3PbI_3$ ($MAPbI_3$) by a reaction with CH_3NH_3I (MAI) in the solution or vapour phase.

Since a compact and uniform perovskite film especially a planar perovskite film is so crucial for the fabrication of high efficiency perovskite solar cells, the controllable growth of the perovskite film especially the planar perovskite film has become the focus for perovskite solar cell research. A fast crystallization or formation of a high quality planar perovskite film is desired to avoid film shrinkage in the one step method or volume expansion in sequential deposition approaches.[17–19] Currently, the most reported successful one-step methods like the famous $CH_3NH_3PbI_{3-x}Cl_x$ (ref. 5) or solvent engineering fabricated $MAPbI_3$ (ref. 3 and 17) are all highly sensitive to humidity levels. Some pioneering studies had already pointed out that it is better to fabricate high quality perovskite films in dry air or a glovebox.[20] A recent report has demonstrated that the morphology of the $FAPbI_3$ planar film prepared *via* solvent engineering can be significantly deteriorated with increasing humidity levels.[21] In comparison, sequential deposition exhibited a better moisture tolerance than the one-step method, and recently Park's group has fabricated a ~15% efficiency perovskite solar cell under ~50% humidity level.[22] It is well known that the growth and film morphology of the final perovskite $MAPbI_3$ *via* sequential deposition is strongly dependent on the PbI_2 precursor film. The sequential deposition's relatively better humidity tolerance could be attributed to the initial PbI_2 precursor film's less sensitivity to moisture. However, for a fast and complete conversion of planar PbI_2 to perovskites, the uniform PbI_2 film is the main challenge. In the first report on sequential deposition of planar $MAPbI_3$, Mitzi and his co-workers had to soak the PbI_2 film in MAI isopropanol solution for hours.[16] Recently some reports have shown that a porous PbI_2 film or lower crystallinity PbI_2 film could be beneficial for a quick conversion in sequential deposition.[23,24] Some novel precursor films such as $HPbI_3$, $PbI_2{\cdot}x$HI, $PbI_2{\cdot}x$MAI or

School of Environmental Science and Engineering, Shanghai Jiao Tong University, 800 Dongchuan Rd., Shanghai 200240, China. E-mail: yixin.zhao@sjtu.edu.cn

† Electronic supplementary information (ESI) available. See DOI: 10.1039/c5ta06172e

‡ GL and TZ contributed equally.

$PbI_2 \cdot x$DMSO have also been developed for a fast perovskite film conversion in sequential deposition.[19,25–27]

In this report, we develop a general stoichiometric usage of HCl for both one-step and sequential deposition methods for preparing compact and uniform planar $MAPbI_3$ films under 60% humidity. The addition of stoichiometric HCl from 33 wt% hydrochloric acid into the one step $MAPbI_3$ DMF precursor solution helps to obtain a dark brown planar $MAPbI_3$ film just after spin coating. The stoichiometric HCl also forms an intermediate precursor film of $HCl \cdot PbI_2$ with PbI_2 when adding 33 wt% hydrochloric acid into the PbI_2 precursor solution. This intermediate film can be completely converted into a planar $MAPbI_3$ film by dipping in MAI isopropanol solution within only 10 s at room temperature. These high quality planar perovskite films deposited by the hydrochloric acid assisted one-step method and sequential deposition method all were successfully used to fabricate ~14% efficiency perovskite solar cells.

Experimental details

Materials

MAI was synthesized by reacting methylamine (MA) with HI, followed by a previously reported purification process.[11,15] A patterned fluorine-doped tin oxide (FTO) was first deposited with a 20 nm thick compact TiO_2 layer by spray pyrolysis of 0.2 M Ti(IV) bis(ethyl acetoacetate)-diisopropoxide 1-butanol solution at 450 °C followed by one hour 450 °C annealing.

One-step deposition of perovskites

A 70 °C freshly prepared perovskite DMF precursor solution of 1.0 M PbI_2 (99.99%) and 1.0 M MAI with the addition of stoichiometric HCl from 33 wt% hydrochloric acid was spin coated onto the 70 °C c-TiO_2 covered FTO substrate at 4000 rpm for 20 s. The obtained dark brownish perovskite film was then annealed at 100 °C for 5 min. All the processes were carried out under a fume hood with ~60% humidity.

Sequential deposition of perovskites

A 70 °C freshly prepared DMF precursor solution of 1.0 M PbI_2 with stoichiometric HCl by adding 33 wt% hydrochloric acid was first spin coated onto the 70 °C patterned FTO at 4000 rpm for 20 s. The deposited film was then immersed into a 10 mg MAI per mL IPA solution for 10 s, followed by rinsing with IPA, blown dry by N_2, and then annealed at 100 °C for 5 min. All the processes were carried out under a fume hood with ~60% humidity.

Device preparation

The perovskite-deposited electrodes were first spin coated with a layer of hole transport material (HTM) of 0.1 M spiro-MeO-TAD, 0.035 M bis(trifluoromethane) sulfonimide lithium salt (Li-TFSi), and 0.12 M 4-*tert*-butylpyridine (tBP) in chlorobenzene/acetonitrile (10 : 1, v/v) solution at 4000 rpm for 20 s. Finally, a 120 nm-thick Ag contact layer was deposited by thermal evaporation, as previously described.[28]

Characterization

The crystal structures of the perovskite films were measured by X-ray diffraction (XRD, Shimadzu XRD-6100 diffractometer with Cu K_α radiation). The morphologies of the planar perovskite films were characterized on a FEI Sirion 200 scanning electron microscope (SEM) with EDX. The absorption spectra of the planar perovskite films were characterized on a Cary-60 UV-vis spectrophotometer. The photocurrent density–voltage (J–V) characteristic of perovskite solar cells was measured with a Keithley 2402 source meter under simulated AM 1.5G illumination (100 mW cm^{-2}; Newport Class AAA Solar Simulator).

Results and discussion

Sequential deposition

The addition of stoichiometric HCl from 33 wt% hydrochloric acid into PbI_2 DMF solution leads to the formation of a smooth green yellowish film, while the typical PbI_2 film is yellowish. As shown in Fig. 1A, the greenish precursor film exhibits an absorbance peak at ~420 nm, which is different from the PbI_2 film's well known characteristic UV-vis absorbance at ~500 nm. The XRD of this greenish film sample exhibited a very strong unknown XRD peak at around 9°as shown in Fig. 1B, which is different from that of PbI_2. These results suggested that the addition of stoichiometric HCl into PbI_2 may have formed a novel precursor. The EDX results reveal that there is Cl found in the novel precursor film, which confirms the incorporation of Cl into the film. Here we note this novel precursor film as $HCl \cdot PbI_2$, which may be similar to the previously reported $HPbI_3$ film.[25] Interestingly, we found that the 100 °C annealing would turn this new $HCl \cdot PbI_2$ precursor film back into the PbI_2 film after 10 min annealing as shown in Fig. S1.† Further EDX measurements revealed that there is no Cl residue found on this annealed sample at 100 °C for 10 min. These results suggested that this $HCl \cdot PbI_2$ is unstable and the HCl composition can be easily removed by annealing.

It is well known that the main difficulty in sequential deposition of planar perovskite films from the PbI_2 precursor film is the relatively slow complete conversion process in the second dipping step. Usually, the initial yellow planar PbI_2 film slowly changes its colour to brown or dark brown depending on the solution temperature and the MAI solution concentration. The slow conversion of planar PbI_2 into perovskite could be attributed to the volume expansion induced inhibited intercalation of MAI into the PbI_2 lattice in planar films.[19] Most of the previously reported planar perovskite films fabricated by sequential deposition need to be dipped in warm MAI solution for more than several minutes or up to an hour at room temperature MAI solution. Interestingly, our greenish $HCl \cdot PbI_2$ precursor film with high crystallinity turns dark brown immediately after dipping into MAI solution and totally converted into $MAPbI_3$ within 10 seconds once dipped in MAI solution at room temperature as shown in Fig. 1. The UV-vis spectrum of this sample shows a typical $MAPbI_3$ absorbance only after around one second dipping in MAI solution, as shown in Fig. 1A. The around one second dipping not only produces the $MAPbI_3$

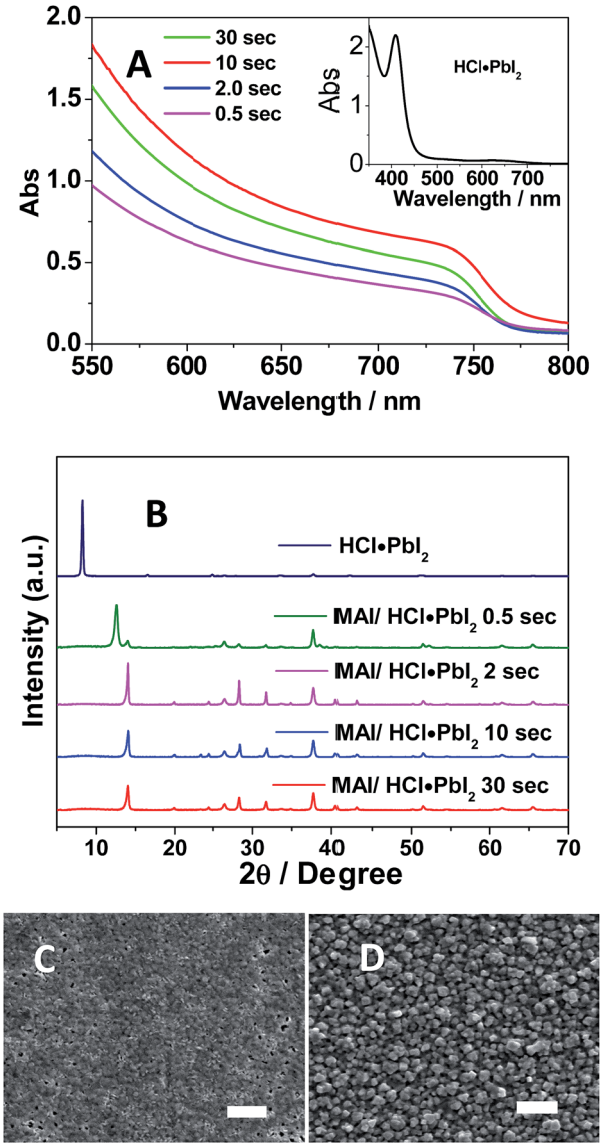

Fig. 1 The dipping time dependent (A) UV-vis absorption spectra and (B) XRD patterns in the 10 mg MAI per mL IPA solution on the evolution of the perovskite films deposited from the planar $HCl{\cdot}PbI_2$ precursor film; the SEM images of the $HCl{\cdot}PbI_2$ precursor film (C) and the resulting $MAPbI_3$ film (D). The scalebar is 1 μm.

perovskite film but also forms the PbI_2 with the total disappearance of the $HCl{\cdot}PbI_2$ film as shown in Fig. 1B. This observation suggests that the $HCl{\cdot}PbI_2$ can be rapidly converted into PbI_2. After 10 second dipping, all the $HCl{\cdot}PbI_2$ and PbI_2 peaks totally disappear, and the absorbance of $MAPbI_3$ reaches the maximum. Both the XRD intensity and UV-vis absorbance of the $MAPbI_3$ perovskite planar film then decrease with a longer dipping time due to the dissolution. In our previous work, we found that it takes more than 6 minutes for the regular planar PbI_2 film to be completely converted into the $MAPbI_3$ film when dipped in a warm MAI solution.[19] Here we can convert the planar $HCl{\cdot}PbI_2$ precursor film into $MAPbI_3$ within 10 seconds in a room temperature MAI solution. This clearly suggests that our $HCl{\cdot}PbI_2$ precursor film can be rapidly converted into $MAPbI_3$.

The SEM images in Fig. 1C and D reveal that the $HCl{\cdot}PbI_2$ precursor film is compact and uniform consisting of small nanocrystals. This is different from the previously reported PbI_2 film, which is usually less smooth and without obvious nanocrystal particles due to its layered structure. The $MAPbI_3$ planar film prepared from the $HCl{\cdot}PbI_2$ film is also compact and full of uniform $MAPbI_3$ nanocrystals. The size of $MAPbI_3$ is similar to that of the $HCl{\cdot}PbI_2$ precursor nanocrystals. The unique small crystal grains of $HCl{\cdot}PbI_2$ may also help the rapid conversion of $MAPbI_3$ besides the unique crystal structure of $HCl{\cdot}PbI_2$. There is no Cl found in the final $MAPbI_3$ film suggesting that the Cl was removed during the sequential deposition. Furthermore, there is ~10% volume expansion found in the $HCl{\cdot}PbI_2$ precursor film and the corresponding perovskite film as shown in Fig. S2.†

One step method

In a standard one-step method without solvent engineering or additives,[1,2,7] it is difficult to obtain a planar $MAPbI_3$ with high coverage by just spin coating a 1.0 M (PbI_2 + MAI) DMF precursor solution. Fig. 2A–C show the UV-vis spectra, XRD patterns and SEM images of a typical regular one step method prepared planar perovskite films with low coverage and crystallinity, which is consistent with previous reports.[15,28–30] Once a stoichiometric HCl from 33 wt% hydrochloric acid was added into 1.0 M (PbI_2 + MAI) DMF solution to form a new precursor solution of (PbI_2 + MAI + HCl), a mirror like smooth perovskite planar film with a dark brown color was formed just after the spin coating. In contrast, the (PbI_2 + MAI) DMF solution prepared film is yellowish after spin coating, which suggested that the presence of HCl may affect the crystallization of $MAPbI_3$. The role of HCl is similar to some previously reported chlorine compounds such as MACl, which assists growth of high quality perovskite films. Unlike the long time annealing to remove the reported chlorine additive, here we found that there is no Cl found even in the film without annealing. This suggests that the HCl could be removed during the spin coating process. However, a 5 minute 100 °C annealing treatment was still carried out immediately after spin coating in order to remove the H_2O introduced by the addition of 33 wt% hydrochloric acid. The UV-vis spectrum of the obtained smooth film is displayed in Fig. 2A, which shows a characteristic $MAPbI_3$ absorbance. The XRD patterns in Fig. 2B also confirm the formation of $MAPbI_3$ perovskite. Furthermore, the XRD peak intensity of one-step method prepared perovskite films from the (PbI_2 + MAI + HCl) prepared sample is much higher than that from regular (PbI_2 + MAI) precursor solution. The SEM image in Fig. 2D reveals that the planar perovskite film is full of compact $MAPbI_3$ nanocrystals without pinhole, which is smoother than the sequentially deposited ones. This suggested that the presence of HCl could significantly promote the crystallization of $MAPbI_3$, which has some similarities to both the solvent engineering and additive one step method. There is no traceable Cl found in our EDX measurements of these one step method prepared perovskite films.

Although previous studies have suggested that the formations of PbI_2 precursor films and $MAPbI_3$ films are all highly

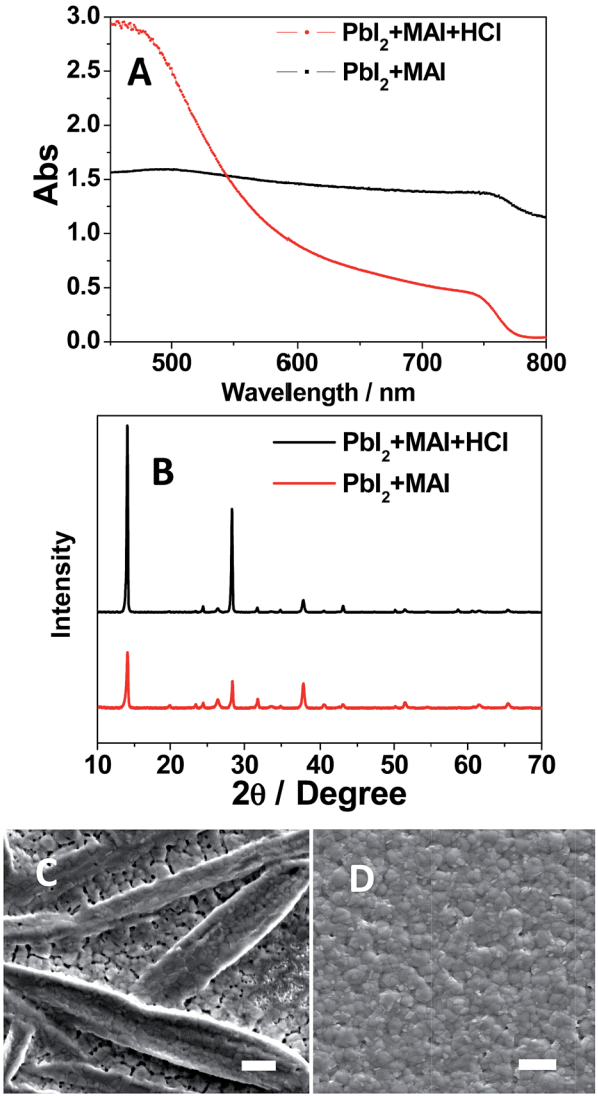

Fig. 2 The UV-vis spectra (A) and XRD patterns (B) of planar $MAPbI_3$ prepared from PbI_2 + MAI and PbI_2 + MAI + HCl precursor solutions by the one step method; the SEM images of the planar $MAPbI_3$ film prepared from (C) PbI_2 + MAI and (D) PbI_2 + MAI + HCl precursor solutions. The scalebar is 1 μm.

sensitive to moisture,[21,22] our new precursor solutions of (PbI_2 + HCl) and (PbI_2 + MAI + HCl) can fabricate very smooth HCl·PbI_2 and $MAPbI_3$ *via* spin coating in a hood under ambient conditions with a humidity level up to 60%. The reason for this high humidity tolerance is that our (PbI_2 + HCl) and (PbI_2 + MAI + HCl) precursors already contain some H_2O by the addition of 33 wt% hydrochloric acid, which makes this precursor solution less sensitive to moisture in air. A previous report has suggested that the Cl has some special interaction with PbI_2.[31] Here we propose that a plausible reason for the high humidity tolerance is that HCl might have more affinity to complex with PbI_2 or $MAPbI_3$ than H_2O to prevent humidity from affecting the perovskite's crystallization process. However, the interaction of HCl with PbI_2 seems much weaker than that of PbI_2 and MAI, which accounts for the ultra-fast conversion of HCl·PbI_2 into $MAPbI_3$ in sequential deposition.

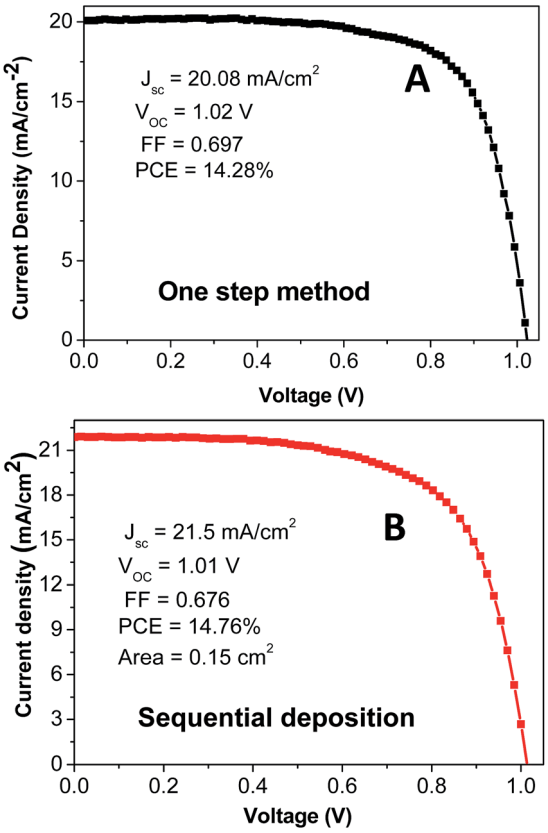

Fig. 3 Typical *J–V* curves of planar $MAPbI_3$ solar cells prepared from our (A) one-step method (PbI_2 + MAI + HCl) and (B) sequential deposition (HCl·PbI_2).

Fig. 3 shows the typical *J–V* characteristics of perovskite solar cells based on the planar $MAPbI_3$ film fabricated from both the one-step method and sequential deposition. The cells' efficiencies are around 14% with a J_{sc} of more than 20 mA cm^{-2}, a V_{oc} of ~1.0 V, and a FF of 0.65–0.70. The sequential deposition fabricated planar $MAPbI_3$ film exhibited a higher J_{sc}, which is consistent with the high absorbance of the sequential deposition prepared $MAPbI_3$ film as shown in Fig. 1 and 2. The sequential deposition fabricated perovskite solar cell generally has a lower FF value, which could be attributed to the more rough morphology compared to the one step method. Due to our device fabrication facility and the planar configuration's intrinsic limitation related to the compact TiO_2 as the electron transfer layer and the usage of spiro-MeOTAD as the hole transfer material, our perovskite solar cells all exhibited a hysteresis as shown in Fig. S3.† But these perovskite solar cells with *J–V* hysteresis exhibited a stable photocurrent of ~17.5 mA cm^{-2} at 0.81 V bias, which suggests a stable efficiency of ~14.1% as shown in Fig. S4.†

Conclusions

In summary, we have developed HCl assisted one-step and sequential deposition methods to accelerate the formation of a pinhole free planar $CH_3NH_3PbI_3$ perovskite film. In these

methods, stoichiometric HCl is added to the standard PbI_2 and $MAPbI_3$ precursor (equimolar mixture of MAI and PbI_2) solution by adding 33 wt% hydrochloric acid. The stoichiometric HCl and PbI_2 could form new unknown $HCl \cdot PbI_2$ precursor films, which can be easily thermally decomposed back into PbI_2. In the sequential deposition, the Cl composition is immediately removed from the $HCl \cdot PbI_2$ film and the precursor film is then converted into $MAPbI_3$ perovskite and PbI_2. This smooth planar $HCl \cdot PbI_2$ nanocrystal film can be completely converted into $MAPbI_3$ without any Cl residue by just dipping in MAI isopropanol solution within 10 s at room temperature. The addition of stoichiometric HCl into MAPbI3 precursor solution helps to form a compact and smooth $MAPbI_3$ film without Cl residues by regular one step spin coating even without annealing. Both the one-step method and sequential deposition with addition of stoichiometric HCl show high moisture tolerance, which can form a smooth perovskite film in a hood under ambient conditions with up to 60% humidity levels. These high quality planar perovskite films prepared *via* HCl accelerated formation can be used to fabricate high efficiency planar perovskite solar cells with a stable output.

Acknowledgements

YZ is thankful for the support from the NSFC (Grant 51372151 and 21303103).

Notes and references

1 A. Kojima, K. Teshima, Y. Shirai and T. Miyasaka, *J. Am. Chem. Soc.*, 2009, **131**, 6050–6051.
2 J.-H. Im, C.-R. Lee, J.-W. Lee, S.-W. Park and N.-G. Park, *Nanoscale*, 2011, **3**, 4088–4093.
3 N. J. Jeon, J. H. Noh, Y. C. Kim, W. S. Yang, S. Ryu and S. I. Seok, *Nat. Mater.*, 2014, **13**, 897–903.
4 J. Burschka, N. Pellet, S. J. Moon, R. Humphry-Baker, P. Gao, M. K. Nazeeruddin and M. Gratzel, *Nature*, 2013, **499**, 316–319.
5 M. M. Lee, J. Teuscher, T. Miyasaka, T. N. Murakami and H. J. Snaith, *Science*, 2012, **338**, 643–647.
6 R. F. Service, *Science*, 2014, **344**, 458.
7 H.-S. Kim, C.-R. Lee, J.-H. Im, K.-B. Lee, T. Moehl, A. Marchioro, S.-J. Moon, R. Humphry-Baker, J.-H. Yum, J. E. Moser, M. Gratzel and N.-G. Park, *Sci. Rep.*, 2012, **2**, 1–7.
8 Y. Zhao and K. Zhu, *J. Phys. Chem. Lett.*, 2014, **5**, 4175–4186.
9 B. Conings, L. Baeten, C. de Dobbelaere, J. D'Haen, J. Manca and H.-G. Boyen, *Adv. Mater.*, 2014, **26**, 2041–2046.
10 P.-W. Liang, C.-Y. Liao, C.-C. Chueh, F. Zuo, S. T. Williams, X.-K. Xin, J. Lin and A. K. Y. Jen, *Adv. Mater.*, 2014, **26**, 3748–3754.
11 Y. Zhao and K. Zhu, *J. Phys. Chem. Lett.*, 2013, **4**, 2880–2884.
12 J. T. Wang, J. M. Ball, E. M. Barea, A. Abate, J. A. Alexander-Webber, J. Huang, M. Saliba, I. Mora-Sero, J. Bisquert, H. J. Snaith and R. J. Nicolas, *Nano Lett.*, 2013, **14**, 724–730.
13 H.-S. Kim, J.-W. Lee, N. Yantara, P. P. Boix, S. A. Kulkarni, S. Mhaisalkar, M. Grätzel and N.-G. Park, *Nano Lett.*, 2013, **13**, 2412–2417.
14 J. H. Noh, S. H. Im, J. H. Heo, T. N. Mandal and S. I. Seok, *Nano Lett.*, 2013, **13**, 1764–1769.
15 Y. Zhao and K. Zhu, *J. Phys. Chem. C*, 2014, **118**, 9412–9418.
16 K. Liang, D. B. Mitzi and M. T. Prikas, *Chem. Mater.*, 1998, **10**, 403–411.
17 M. Xiao, F. Huang, W. Huang, Y. Dkhissi, Y. Zhu, J. Etheridge, A. Gray-Weale, U. Bach, Y.-B. Cheng and L. Spiccia, *Angew. Chem., Int. Ed.*, 2014, **53**, 9898–9903.
18 E. D. Gaspera, Y. Peng, Q. Hou, L. Spiccia, U. Bach, J. J. Jasieniak and Y.-B. Cheng, *Nano Energy*, 2015, **13**, 249–257.
19 T. Zhang, M. Yang, Y. Zhao and K. Zhu, *Nano Lett.*, 2015, **15**, 3959–3963.
20 G. E. Eperon, V. M. Burlakov, P. Docampo, A. Goriely and H. J. Snaith, *Adv. Funct. Mater.*, 2014, **24**, 151–157.
21 S. Wozny, M. Yang, A. M. Nardes, C. C. Mercado, S. Ferrere, M. O. Reese, W. Zhou and K. Zhu, *Chem. Mater.*, 2015, **27**, 4814–4820.
22 H.-S. Ko, J.-W. Lee and N.-G. Park, *J. Mater. Chem. A*, 2015, **3**, 8808–8815.
23 Y. Zhao and K. Zhu, *J. Mater. Chem. A*, 2015, **3**, 9086–9091.
24 Y. Wu, A. Islam, X. Yang, C. Qin, J. Liu, K. Zhang, W. Peng and L. Han, *Energy Environ. Sci.*, 2014, **7**, 2934–2938.
25 F. Wang, H. Yu, H. Xu and N. Zhao, *Adv. Funct. Mater.*, 2015, **25**, 1120–1126.
26 W. S. Yang, J. H. Noh, N. J. Jeon, Y. C. Kim, S. Ryu, J. Seo and S. I. Seok, *Science*, 2015, **348**, 1234–1237.
27 J.-H. Heo, H. J. Han, D. Kim, T. Ahn and S. H. Im, *Energy Environ. Sci.*, 2015, **8**, 1602–1608.
28 Y. Zhao and K. Zhu, *J. Am. Chem. Soc.*, 2014, **136**, 12241–12244.
29 Y. Chen, Y. Zhao and Z. Liang, *Chem. Mater.*, 2015, **27**, 1448–1451.
30 Y. Chen, Y. Zhao and Z. Liang, *J. Mater. Chem. A*, 2015, **3**, 9137–9140.
31 H.-S. Kim, S. H. Im and N.-G. Park, *J. Phys. Chem. C*, 2014, **118**, 5615–5625.

